Structural Behavior of Shear Wall Strengthened by Carbon FRP Strips Mechanically Fastened under Cyclic Lateral Load

Mohamed H. Agamy [1], Alaa Eldin M. Sileem[2,*], Nehal M. Abd Elaziz [1], Mohamed Salem [3]

[1] Helwan University - Faculty of Engineering - Department of Civil Engineering – Egypt

[2]Higher Institute of Engineering-Institute of Civil and Architecture Engineering -15May City-Egypt

[3] Housing and Building National Research Center-Egypt

[*]Corresponding author E-mail: aladinsleeem @gmail.com

Abstract. This study investigates the structural behavior of shear walls strengthened externally with mechanically fastened carbon fiber reinforced polymer (CFRP) strips under cyclic loads. Five specimens, each featuring distinct strengthening configurations (SHW0, SHW1, SHW2, SHW3, and SHW4), were examined; the specimen SHW0 is serving as the control sample and the others have been strengthened with carbon fiber Reinforced Polymer (CFRP) strips, using both mechanical fasteners and non-fastened methods. The results demonstrated that the addition of CFRP strips significantly enhances the load-bearing capacity, displacement resistance, ductility, and energy dissipation of the shear walls. Specifically, SHW3 merges horizontal CFRP strips with mechanical fasteners, exhibited the highest performance in terms of load capacity, ductility, and energy absorption. SHW4, with CFRP X-strips and fasteners, followed closely behind. In contrast, SHW1 and SHW2, although showing improvement over SHW0, offer lower levels of deformation capacity and energy dissipation. Furthermore, mechanical fasteners play a critical role in enhancing the energy dissipation capacity and stability of shear walls under seismic loads.

Keywords: Shear walls, CFRP, strengthened, mechanically fastened, cyclic load, quasi-static lateral load.

1. Introduction

Shear walls are popular lateral load-resisting methods used in many reinforced concrete (RC) structures designed for earthquake resistance. A restricted number of reinforced concrete shear walls is used in older structures. It was found that the walls of some buildings had cross sections with low aspect ratios (h/l, where h is the wall's height and l is its length), which sometimes looked like rectangular elongated columns. These structures endured the earthquake with minimal damage to the structural frame system but substantially harmed the masonry walls [1]. In these buildings, inadequately built and

detailed shear walls, which sustained diagonal shear cracks, endured the earthquake and preserved the structure. The shear cracks observed in the shear walls were sufficiently wide to suggest the possible yielding of the reinforcements. Moreover, there were existing older structures that were constructed with markedly worse concrete quality. Despite the extensive damage to the concrete in these walls, the shear walls protected the structures and prevented collapse. A substantial proportion of existing structures are constructed so that shear walls support only vertical loads, excluding lateral loads. The shear walls of various existing buildings exhibit multiple design and construction detail deficiencies, including insufficient or absent confinement of boundary elements with adequate reinforcement, inadequate bonding of transverse reinforcement to concrete, and insufficient shear strength to prevent the development of hinging. As a result, enhancing the shear capability of reinforced concrete walls has been a primary priority in the earthquake-resistant construction of reinforced concrete structures. The strengthening of shear-deficient concrete walls considerably increases seismic structural performance.

In the past decade, there has been a substantial increase in the strengthening of reinforced concrete (RC) structures using fiber-reinforced polymers (FRPs), largely ascribed to their simplicity of application, improved corrosion resistance, and high strength-to-weight ratio. Research focuses mainly on reinforced concrete columns strengthened by fiber-reinforced polymer jackets [1–3]. However, investigations of RC walls strengthened using fiber-reinforced polymer sheets are limited in amount. One of the earliest experimental tests on the strengthening of reinforced concrete (RC) walls involves the installation of fiber-reinforced polymer (FRP) sheets vertically on the wall sides to counteract cyclic shear and flexure [4-13]. Another study explores various strengthened configurations of externally bonded FRP applied to walls, comparable to columns under uniaxial compression. [4-13]. Additional studies involve the usage of wing walls on reinforced concrete columns and their application on unreinforced concrete infill walls [14-16].

Despite the ease and practicality of using FRP strips to improve shear-deficient reinforced concrete walls, little research has been conducted on the impact of strip patterns on hysteretic behavior. The primary goal of this study is to experimentally evaluate acceptable CFRP strip configurations for improving the hysteretic performance of shear-deficient reinforced concrete walls under cyclic lateral loads. The primary experimental variable investigated in this study is the effect of four CFRP strip configurations: horizontal strips, X-shaped strips, a combination of X-shaped and horizontal strips, and a blend of X-shaped and parallel strips in shear-deficient reinforced concrete walls strengthened under cyclic lateral loading tests. Furthermore, the study investigates the lateral load-displacement characteristics, strength, ductility, energy dissipation, and failure mechanisms of reinforced concrete walls strengthened using CFRP strips.

2. Experiment Program

2.1. Test Parameters

The main parameters examined in the experimental program are the following:
1. Axial loading (N = 70 kN), calculated according to ACI-318 [17].
2. CFRP strips configuration (X-shape, longitudinal).
3. CFRP stirps bonding with concrete (mechanical fasteners, epoxy resins)

The details of wall specimens are shown in Fig. 1.
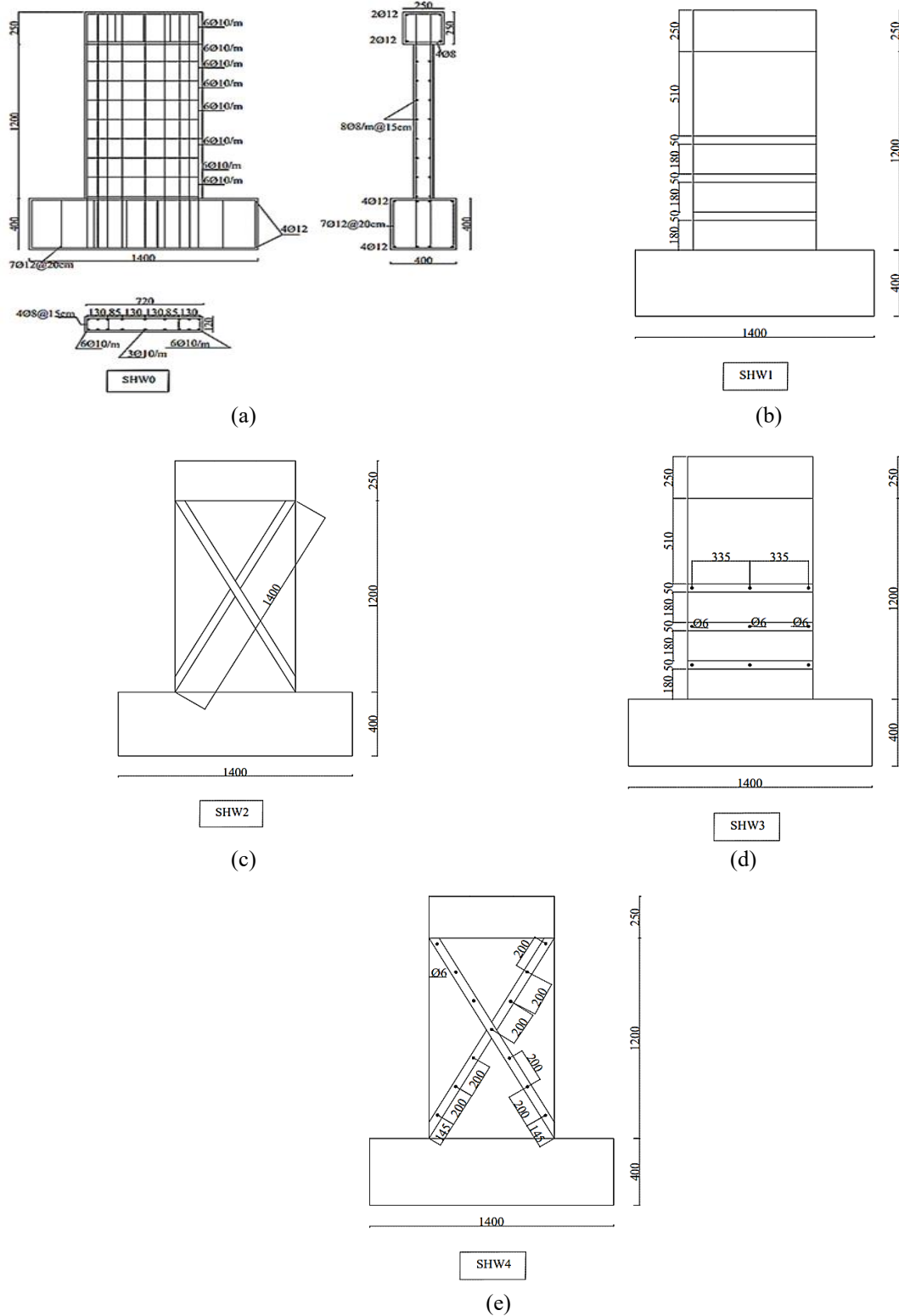
Fig. 1: The dimensions and reinforcement of wall specimens; (a) SHW0, (b) SHW1, (c) SHW2, (d) SHW3, and (e) SHW4.

2.2. Tested Specimens

Five samples of shear walls with varying CFRP configuration sections are studied. The sample 'SHW0' is utilized as the control specimen for monolithic reinforced concrete. The samples had been created to represent a prototype shear wall utilized in structures. The test specimens feature a rectangular cross section of 720×120 mm. Fig. 1 displayed the configurations of CFRP for walls. The parameters investigated included the utilization of different shapes of CFRP configurations in the wall's sections. The magnitude of the applied axial stresses was determined as 0.10 of the nominal axial compressive strength (P_n = 230 kN) [17]. The test specimens include a portion of a shear wall of an existing aged structure. Five half-scale concrete shear wall specimens that had been strengthened were produced and tested in the laboratory of HBRC to explore the effect of shear strengthening obtained by four various CFRP configurations on the hysteretic behavior of structural shear walls. The dimensions and strengthening characteristics of the tested samples are shown in Fig. 1. All test items share similar geometrical dimensions and strengthening configurations. The samples contain three structural components: the head beam, which transmits lateral stresses to the wall; the panel, which resembles a shear wall; and the footing, which ties the specimen to the laboratory's hard floor

The head beam has a cross-sectional dimension of 250 mm by 250 mm. The vertical and stirrups reinforcement of the beam head are 4Φ12mm and 5ϕ8mm/m′, respectively.

The footing has a cross section of 400 mm x 400 mm and a length of 1400 mm. The footing is reinforced with two layers of 4Φ12mm in short direction and 7Φ12mm in the other direction.

The dimensions of the wall are length (l) = 720mm, height (h) = 1200 mm, and thickness (t) = 120 mm. The wall aspect ratio (h/l) is 1.67. The wall's lateral and vertical reinforcement has two levels. Vertical uniform reinforcements with a diameter of 10mm are used, spaced at 130 mm. The concentrated vertical reinforcement on both sides of the wall has six 10mm diameter deformed bars. This approach enhances the flexural capacity of the wall, which requiring an improvement in shear strength. The SHW0 sample served as the reference specimen tested without strengthening. The remaining four specimens (Specimens SHW1– SHW4) underwent tested after strengthening with four different configurations of CFRP strips. CFRP strips were symmetrically affixed to both sides of the concrete wall. Fig. 1 provides comprehensive descriptions of the CFRP configurations implemented. Lateral strips, 50 mm in width and positioned 180 mm apart, were applied strengthen the specimen SHW1. CFRP strips, 50 mm in width, were laid diagonally in an X-shape over the walls of the specimen SHW2. Specimen SHW3 was strengthened with lateral CFRP strips with mechanical fasteners with 6mm diameter and length 6cm at 330 mm spacing. The specimen SHW4 was strengthened by X-strips with mechanical fasteners with 6mm diameter and length 6cm at 200 cm distance for each. All specimens were cast horizontally on the laboratory floor. The samples have been constructed in two phases. In the initial phase, the reinforced concrete shear wall was cast and hardened for 28 days. During the second phase, the specimens were strengthened using CFRP. To achieve this purpose, the locations of CFRP strips and fasteners were determined on the specimens as an initial stage. Subsequently, anchoring holes with a diameter of 6 mm were bored and the wall surfaces specified for the bonding of CFRP strips were roughened to ensure an appropriate bonding surface for CFRP strips. The surfaces and anchor holes had been cleared of dust using compressed air, followed by the use of epoxy to the surfaces at a thickness of 1.5 mm and its injection into the anchor holes. Subsequent to the affixation of CFRP strips to the walls.

2.3. Material Property

The shear wall specimens were manufactured and tested in the Reinforced Concrete Laboratory of HBRC. The concrete used was mixed in the laboratory mixing plant. To determine the average compressive strength of concrete, three cubes (150×150×150 mm) were evaluated for each specimen. The assessed concrete compressive strength was around 35 MPa, which correlates to a cylinder compressive strength of 26 MPa. The mean mechanical characteristics of steel were determined by

testing three samples of reinforcing steel bars for each nominal diameter, whereas CFRP strip values were obtained from the supplier. The characteristics of the steel reinforcement and CFRP are provided in Tables 1 and 2.

Table (1): Material properties for reinforcing bars

Material	Yield strength, f_y (N/mm^2)	Ultimate strength, f_u (N/mm^2)
Stirrups Ø 8	448	507
Bars Φ 10	554	700
Bars Φ 12	592	738

Table (2): Material properties for CFRP

Properties of CFRP	Remarks of CFRP
Thickness (mm)	1.2
Tensile strength (MPa)	2800
Elastic modulus (MPa)	165000
Ultimate tensile strain (%)	1.7%
Properties of resin	**Remarks of CFRP**
Tensile strength	30
Elastic modulus	12800

2.4. Test Set-up

The full test configuration for cyclic loading is illustrated in Fig. 2. To prevent elevation during the application of cyclic loads, each sample was anchored to the floor of the laboratory by prestressing steel bars. A hydraulic jack was used to apply an axial load to the head beam of the shear wall for each specimen, which remained constant. Hydraulic actuators were used to apply cyclic loading over the top beam. The cyclic hydraulic actuator can handle ±250kN in compression and tension.

Fig. 2: Cyclic loading test set-up.

2.5. Instrumentation

The data collection system consists of four internal control and recording channels for monitoring data from external LVDTs. In addition to the load cells at the ends of the hydraulic actuators, a number of LVDTs were utilized to measure crucial response values, with one LVDT installed at the top of the specimen to record cyclic displacement. A second one was mounted on the base to record the sliding of the base. Finally, two more LVDTs were installed diagonally on either side of the wall to measure wall cracks. The strains in the CFRP strips were also measured with strain gauges. Fig. 3 depicts the position of the LVDTs.
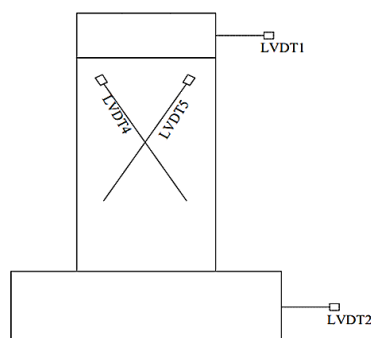
Fig. 3: LVDTs location of typical specimens.

2.6. Application of Cyclic Loading

The samples' tops were loaded horizontally (Fig. 2). Except for the first cycles in the elastic range, displacement control was used during the test. Seventy-five percent of the maximum strength can be used to characterize the normal displacement history up to the failure point. As shown in Fig.2, the shear wall was laterally subjected to a prescribed cyclic displacement history. For SHW0, SHW1, SHW2, SHW3, and SHW4, cyclic displacement of equal positive and negative displacement was used. in accordance with ACI 318 [17]. During all of the tests, the axial stress applied to the wall was equivalent to 0.10Pn. To determine whether the specimen was yielding, the load-lateral displacement hysteresis curve and the structural steel strain state were examined.

3. Test Results

3.1. Crack Patterns and Failure Modes

Shear wall failure modes with and without CFRP strips in different configurations include brittle shear failure at the wall's diagonals and concrete spalling at the wall's base. In Fig. 4, the failure modes are shown.

For sample SHW0, shear cracks appear at 14 mm displacement at the diagonals of the shear wall. With extra rise of external load, intersectional shear cracks occurred in the wall zone. Furthermore, it failed due to brittle shear cracks of the concrete at 40 mm displacement.

SHW0 images indicate extensive cracking, spalling, and concrete crushing, notably in the lowest regions of the shear wall. This damage suggests a flexural-shear failure mechanism. Diagonal cracks are prominent in the central region, extending towards the edges, indicating shear deformation. Horizontal cracks nearby the base, showing flexural failure, where bending loads exceed the wall's capacity to withstand them. Vertical cracks show axial load effects, leading to reduced stiffness. Concrete Crushing: Severe concrete crushing is found near the bottom, showing compressive failure in the compression zone. Pinching Effect Relation to harm.

In the upward displacement direction (tensile side) the maximum load is approximately 105kN.The optimum displacement in the upward direction (tensile) is 40 mm, which relates to the maximum elongation of the wall before serious degradation begins.

The maximum load in the downward displacement direction (compressive side) is roughly 160 kN, the optimal displacement in the downward direction (compressive) is -30 mm, illustrating the highest compression the wall withstood before catastrophic collapse occurred.

The maximum load is approximately 105kN when displaced upwards (tensile side). The optimum upward displacement (tensile) is 40 mm, which corresponds to the maximal wall elongation before severe degradation occurs.

The maximum load in the compressive side (downward displacement direction) is around 160 kN, and the ideal compressive displacement is -30 mm. These values show the maximum compression the wall could withstand prior to a catastrophic collapse.

For sample SHW1, the shear cracks form at 10.52 mm displacement at the diagonals of wall. With increased displacement, more shear cracks appeared in the diagonal region and back CFRP raptured at 22.02mm and the cover of concrete crushed at 28.58mm. Finally, specimen SHW1 failed at a displacement of 33.88mm due to a shear crack of concrete in the diagonal zone.

SHW1 has significant cracking and crushing of the concrete, particularly at the shear walls' bottom. This indicates that SHW1 experienced a flexural-shear failure mechanism that was similar to SHW0, with a few minor adjustments caused by the additional CFRP strips. In the center of the wall, diagonal cracks are found, and they enlarge toward the edges. These cracks are indicative of shear deformation that occurs in the wall. The shear failure mechanism is observable because to the stresses pressing across the wall during cyclic loading.

Horizontal cracks nearby the base suggest flexural failure, with the tension zone being at the wall base where bending forces are strongest. The usage of CFRP strips at the base undoubtedly slowed the start of these cracks, but the appearance of horizontal cracks still suggests flexural instability. Vertical cracks are also seen, primarily around the core region, indicating axial stress effects. The drop in wall stiffness is plainly obvious in the images, as these cracks reduce the wall's capacity to efficiently withstand axial and shear loads. Compressive failure is indicated by the significant concrete crushing around the wall's base. While CFRP strips serve to spread stresses and delay crushing, the wall nevertheless experiences localized failure in the compression zone at high loads.

Few cracks appeared in the SHW2 sample at the start of the test. The shear crack occurs at 14.49mm, with increasing displacement, shear cracks occurred in the diagonal zone and front CFRP raptured at 41mm and back CFRP raptured at displacement 47 mm. Finally, SHW2 collapsed owing to brittle concrete shear fracture at end of at 47 mm displacement. The "X"-shaped CFRP strips that are used for strengthening SHW2 modify the shear wall's overall performance. A controlled propagation of diagonal cracks across the shear wall was significantly affected by the X-shaped CFRP strips.

These cracks are apparent across the wall, showing shear deformation under lateral stress. Unlike SHW0, where shear cracks were more confined, SHW2's reinforcing helped disperse these cracks more equally across the specimen. Horizontal cracks form toward the bottom, which is indicative of flexural collapse. However, the presence of CFRP strengthening likely delayed the initiation of these cracks compared to SHW0, and their progression is less severe, suggesting that strengthening helped resist bending stresses There are vertical cracks around the shear wall base, similar to SHW1, showing axial load effects.

The concrete in this region was exposed to compression and tension forces, but has improved its ability to withstand axial loading. While there is some crushing of concrete at the bottom of SHW2, comparable to SHW1 and SHW0, the extent of damage is minimized.

This demonstrates that the specimen SHW2 benefited from the CFRP strips in the compression zone. The pinching effect seen in the hysteretic curve can be indicative of the same phenomenon observed in SHW1, though to a lesser extent Crack Closure and Reopening.

SHW2's hysteresis loop narrows around zero displacement, showing that fractures close during unloading and reopen during reloading. However, compared to SHW0, the application of CFRP strengthening produced wider hysteresis loops, indicating that CFRP strengthening has enhanced the shear wall's ability to dissipate energy. The pinching effect indicates that there are still signs of slippage in the hysteresis curve, even if the bond between the CFRP strips and the concrete appears to be strong. This demonstrates that there is still considerable bond slip, particularly under higher cycle loads, even with CFRP strengthening.

The peak load in the positive displacement direction (tensile side) is 160 kN, up from SHW0 (105 kN) and SHW1 (150 kN), which indicates that CFRP strips greatly improve the wall's tensile resistance.

Similar to SHW0 and SHW1, the maximum positive displacement is 35 mm, although strengthening increases load resistance. CFRP strips allow the shear wall to sustain greater compressive loads than SHW0 (160 kN) and SHW1 (160 kN). The maximum load in the negative displacement direction (compressive side) is 170 kN. The maximum negative displacement is -40 mm, somewhat higher than SHW0 and SHW1, indicating increased compressive failure resistance.

For SHW3, the initially limited crack formed at the boundary of the wall at the diagonal wall. Shear cracks formed in the joint zone at a displacement of 7 mm. No obvious raptures occurred at horizontal CFRP with fasteners. Finally, the failure of SHW3 was caused by the full development of a plastic hinge at the bottom of the beam at 50 mm displacement. In SHW3, the failure mechanism demonstrates a combination of flexural and shear damage, similar to previous samples, however, the mechanical fasteners paired with CFRP strengthening greatly enhance its behavior under cyclic load.

Mechanical fasteners are crucial in providing a secure connection of CFRP strips to concrete. This results to an increased load transfer between the CFRP and the concrete, which helps prevent debonding under cyclic loads. The fasteners ensure that the CFRP strips remain effectively linked to the concrete, increasing both the shear and tensile resistance of the wall this leads to a more similar cracking distribution, notably in the shear zone, which in SHW3 is more controlled and dispersed across the wall compared to SHW0. These are the major cracks in SHW3, extending in a diagonal pattern, affected by shear deformation. CFRP strips, especially when mechanically connected, help control crack development, leading to more evenly distributed shear damage in the specimen. The fasteners help ensure that the CFRP performs its intended function, limiting premature cracking in the shear zone. Horizontal cracks are more delayed and less extensive in comparison with SHW0 because of the greater resistance to bending given by CFRP strengthening and mechanical fasteners. The technique minimizes the flexural failure at the foundation and helps the shear wall resist bending forces more efficiently.

Similarly to SHW1, vertical cracks near the base indicate axial load impacts, but CFRP strengthening and mechanical fasteners ensure that the cracks do not propagate as quickly or extremely, boosting the compressive capacity of the wall and improving the axial load resistance. The crushing of the concrete near the base is less extreme in SHW3 than in SHW0, demonstrating that the CFRP strengthening, when mechanically secured, greatly decreases the compressive failure. Mechanical fasteners serve to keep the CFRP strips securely linked, thus enhancing the compression resistance in the critical zone. SHW3 has a maximum tensile load of 180 kN, higher than SHW0 (105 kN), SHW1 (150 kN), and SHW2 (160 kN). This increase is caused by the mechanical fasteners that ensure CFRP strength remains securely attached under cyclic loading, helping the shear wall to resist the extra tensile load without failure.

The largest displacement in the positive direction is 45 mm, indicating that SHW3 can tolerate greater deformations before encountering a major loss in strength, thanks to the stability given by CFRP strips and mechanical fasteners. SHW3 has a maximum compressive load of 200 kN, higher than SHW0 (160 kN), SHW1 (160 kN), and SHW2 (170 kN). Mechanical fasteners serve a key role in preventing debonding in the compression zone, where concrete is more sensitive to crushing. This leads to higher compression resistance and helps the shear wall function under compressive stresses. The maximum displacement in the opposite direction is -45 mm, suggesting an enhanced ability to endure compressive failure when compared to SHW0 and SHW1, where the damage in the compression zone was more severe.

The first shear crack in sample SHW4 occurred at an 11 mm displacement, and there were no visible raptures at the X-CFRP fasteners. In the end, SHW4 failed due to complete development at 34 mm displacement. The SHW4 shear wall, consisting of CFRP strips arranged in a "X" diagonal pattern and supported by mechanical fasteners, demonstrates unique damage characteristics compared to the other specimens (SHW0, SHW1, SHW2, and SHW3). The crack distribution pattern in SHW4 is determined by the fasteners used. The SHW4's cracking pattern is notably visible in its X-shaped diagonal cracks. The cracks propose a shear failure, as shear stresses are more obvious approaching the wall's core. The X-shaped pattern indicates shear deformation, but it also shows the force was distributed more uniformly by CFRP and mechanical fasteners, which delayed the start of these deformations. SHW4 cracks are more closely monitored than those in SHW0 and SHW1, which were more widely spread, thanks to mechanical fasteners that prevented premature crack opening and improved the concrete's bearing capacity. There is a lot of spalling on SHW4, especially near the anchor points. Where the fasteners are used. This demonstrates localized compression failure; yet, the application of CFRP strengthening combined with mechanical fasteners appears to have improved shear resistance and avoided the start of complete crushing. The base region shows some concrete separation where the fasteners were installed, indicating a bond failure between the fasteners and the concrete. This detachment could have been caused by localized stress concentrations, which could have been avoided with even more cautious fastener placement. Mechanical fasteners appear to have a key effect in keeping the connection between the CFRP strips and the concrete, preventing the typical debonding failure seen in SHW1 and SHW2. The fasteners reduce CFRP slippage, improve load transmission through reinforced concrete, and enhance overall structure ductility. SHW4 has significantly higher tensile and compressive load capacity compared to other samples. The maximum tensile load is roughly 220 kN, and the maximum compressive load is around 190 kN, which is higher than SHW0 (160 kN), SHW1 (180 kN), SHW2 (~170 kN), and SHW3. The positive displacement is around 50 mm, but the negative displacement is at 45 mm, exhibiting greater ductility and energy dissipation.

(a) SHW0, shear failure attached with spalling of concrete due to yield of bottom reinforcement

(b) SHW1, shear failure at horizontal CFRP with spalling of concrete

(c) SHW2, shear failure at X-CFRP with spalling of concrete

(d) SHW3, shear failure at horizontal CFRP with fasteners

(e) SHW4, shear failure at X CFRP With fasteners
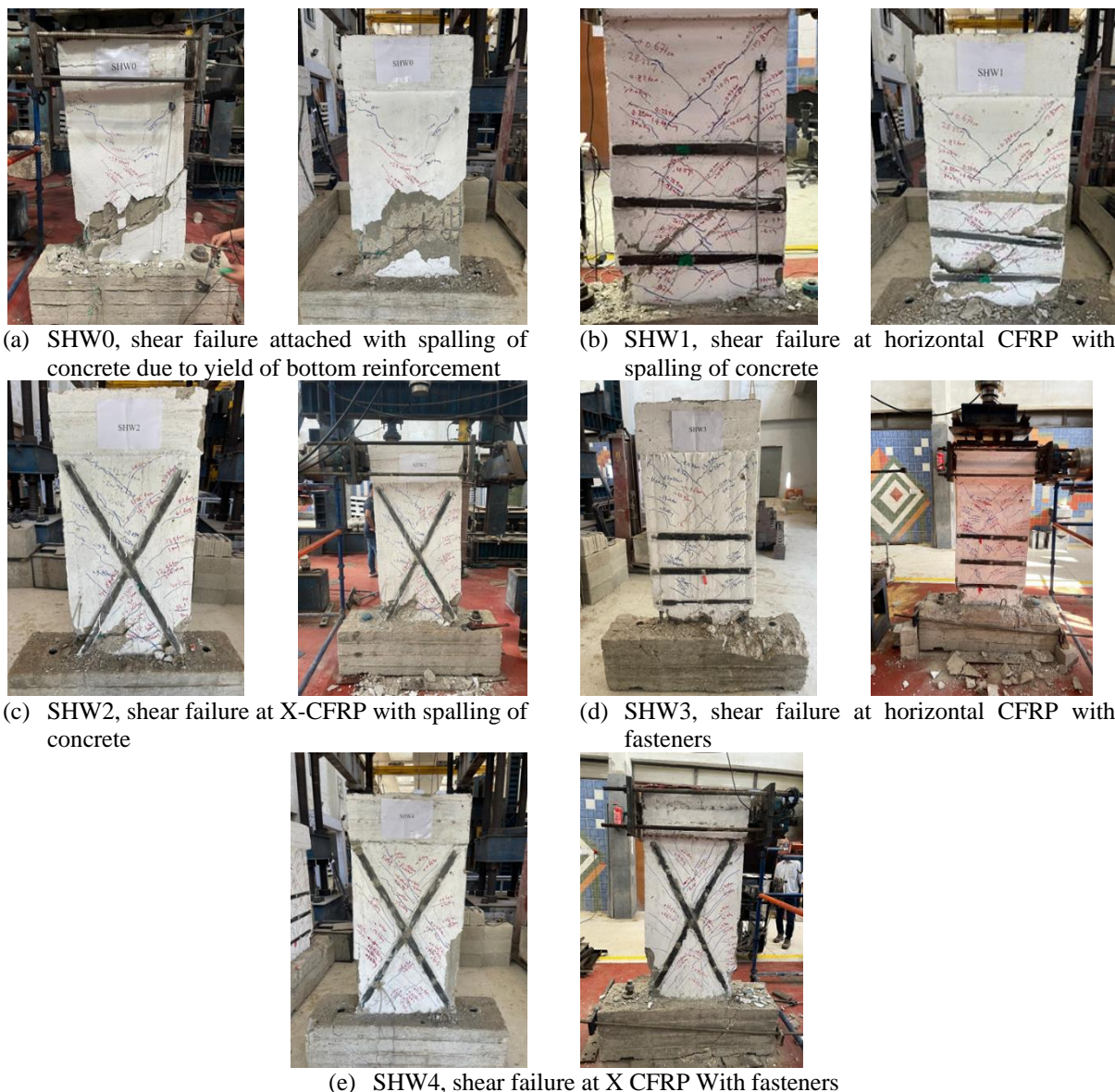
Fig. 4: Failure modes of shear walls without/with different configurations CFRP strips.

3.2. Hysteretic Curve

Figure (6) shows the load-displacement hysteretic responses of the specimens. The hysteresis curve is crucial for understanding the cyclic behavior of structural parts under load, especially in materials and constructions subjected to repeated loading and unloading, such as shear walls. It demonstrates the relationship between the applied load and the resulting displacement in cycle tests. The area inside the loop indicates the energy dissipated during the cycle, and the shape of the curve provides crucial details on the material's stiffness, strength, and ductility under cyclic load. Understanding the hysteresis curve for reinforced structures such as shear walls helps in the research of their behavior in earthquake-like loading scenarios in which elements are subjected to reverse loading cycles, thereby assisting in the construction of more durable structures. The curve gives information on damage mechanisms, including crack development, bond degradation, and stiffness loss, which are useful for evaluating the stability of the structure under future loads. Comparing the hysteresis curves of four specimens (SHW1, SHW2, SHW3, and SHW4) to the control sample (SHW0), it is obvious that adding CFRP strips, with or without fasteners, greatly improves the load-bearing capacity and displacement resistance of shear

walls. SHW0 (control sample) had a maximum positive load of 150 kN and a maximum negative load of -180 kN. The displacement was 45 mm upward (tension) and -50 mm in the opposite direction (compression). The hysteresis curve for SHW0 indicates a large decrease of stiffness after numerous loading cycles, with a pinched shape that is especially noticeable when the load drops, indicating significant energy dissipation and breaking.

SHW1 (horizontal CFRP strips without fasteners) performed substantially better, with a maximum positive load of 170 kN (about 13% higher than SHW0) and a maximum negative load of -210 kN (about 17% higher). The highest displacements were 50 mm (positive) and -55 mm (negative), suggesting that the CFRP strips provided increased displacement resistance. SHW1 has a broader hysteresis loop than SHW0, indicating less pinching and better energy dissipation, particularly during the compression phase.

SHW2 (CFRP X-strips without fasteners) was superior to SHW0, achieving a maximum positive load of 180 kN and a negative load of -220 kN. The maximum upward displacement was 52 mm, while the reverse displacement was -57 mm. The hysteresis loop for SHW2 is substantially wider and smoother than that of SHW0, indicating less stiffness deterioration and more energy absorption.

SHW3 (horizontal CFRP-strips with fasteners) showed an even greater increase, with a maximum positive load of 200 kN (33% higher than SHW0) and a maximum negative load of -250 kN (39% higher). The maximum upward displacement was 55mm, while the reverse direction was -60mm. SHW3's hysteresis curve is significantly more stable, with less pinching, indicating that mechanical fasteners permitted a more uniform distribution of stress across CFRP strips, resulting in a higher overall load capacity and increased displacement resistance.

SHW4 (CFRP X-strips with fasteners) were better than SHW0, with a maximum positive load of 220 kN (47% higher) and a negative load of -260 kN (44% higher). The maximum upward displacement was 58 mm, while the reverse displacement was -65 mm. The SHW4 hysteresis loop's larger and more linear shape indicates higher load-bearing capacity and displacement resistance, attributed to the combined action of CFRP X-strips and fasteners.
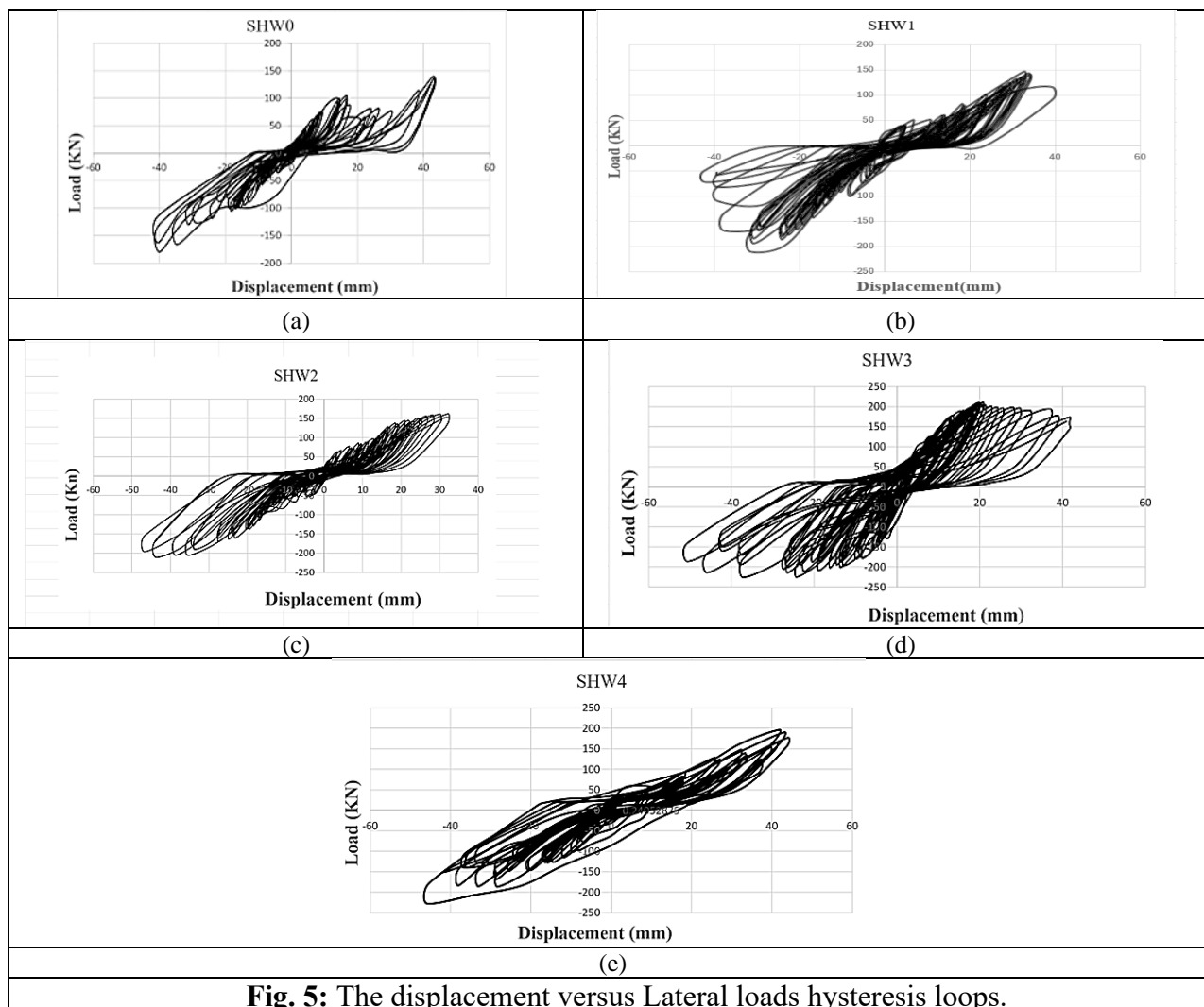
Fig. 5: The displacement versus Lateral loads hysteresis loops.

3.3. Skelton Curve

The skeleton curve is an essential graphical representation utilized in structural analysis to illustrate a system's response to cyclic loading. The highest displacement associated to the highest load achieved during each cycle is presented, thereby showing the overall deformation and energy dissipation of the system. The skeleton curve is necessary to understand the capacity, stiffness degradation, and ductility of the specimen. It aids in analyzing structural behavior, including both elastic and plastic reactions under lateral stresses.

In regard to each of the samples tested (SHW0, SHW1, SHW2, and SHW4), the skeleton curves demonstrate major changes in the load-displacement response, highlighting the impacts of strengthening techniques, such as CFRP strips and mechanical fasteners.

For SHW0 (the control sample), the maximum load reached around 150 kN in upwards, which is with a highest displacement of 40 mm. The curve shows a relatively stable response but with significant stiffness degradation after reaching the maximum load. The envelope is characterized by smaller energy dissipation capabilities, with a smooth slope showing gradual softening.

In SHW1, the maximum load increased to 180 kN, representing a 20% improvement over SHW0. The displacement at the highest load was 50 mm, which is an increase of 25% in comparison with SHW0. This improvement is attributed to horizontal CFRP strips with no mechanical fasteners, as they improved the load-carrying capacity. The skeleton curve shows an initial steeper slope, which leads to a gradual drop, indicating improved energy dissipation before failure.

For SHW2, with CFRP strips arranged in a "X" pattern with no mechanical fasteners, the maximum load was 200 kN, a 33% increase over SHW0, and the largest displacement was 55 mm, a 37.5% rise. The skeleton curve for SHW2 shows a considerable increase in both strength and displacement, indicating higher ductility and improved overall performance compared to SHW0. The curve demonstrates a notceable change in stiffness at higher displacements, indicating a more stable and resilient construction. In SHW3, the sample strengthened with CFRP strips in the "X" pattern and secured with mechanical fasteners showed the highest performance, reaching a maximum load of 220 kN and a maximum displacement of 60 mm. This is a 47% increase in load and a 50% increase in displacement relative to SHW0. The skeleton curve for SHW3 is more obvious exhibiting good strength retention and enhanced energy dissipation, due primarily to the additional anchoring of the CFRP strips. This configuration provided the greatest resistance to deformation.

In comparison, SHW4, with the identical "X" design of CFRP strips and mechanical fasteners, obtained a maximum load of 200 kN and a displacement of 50 mm, similar to SHW2, but with small differences in the curve shape and energy dissipation. The development in strength and displacement was reduced compared to SHW3, showing that the specific mechanical fastening configuration in SHW3 contributed to superior results.
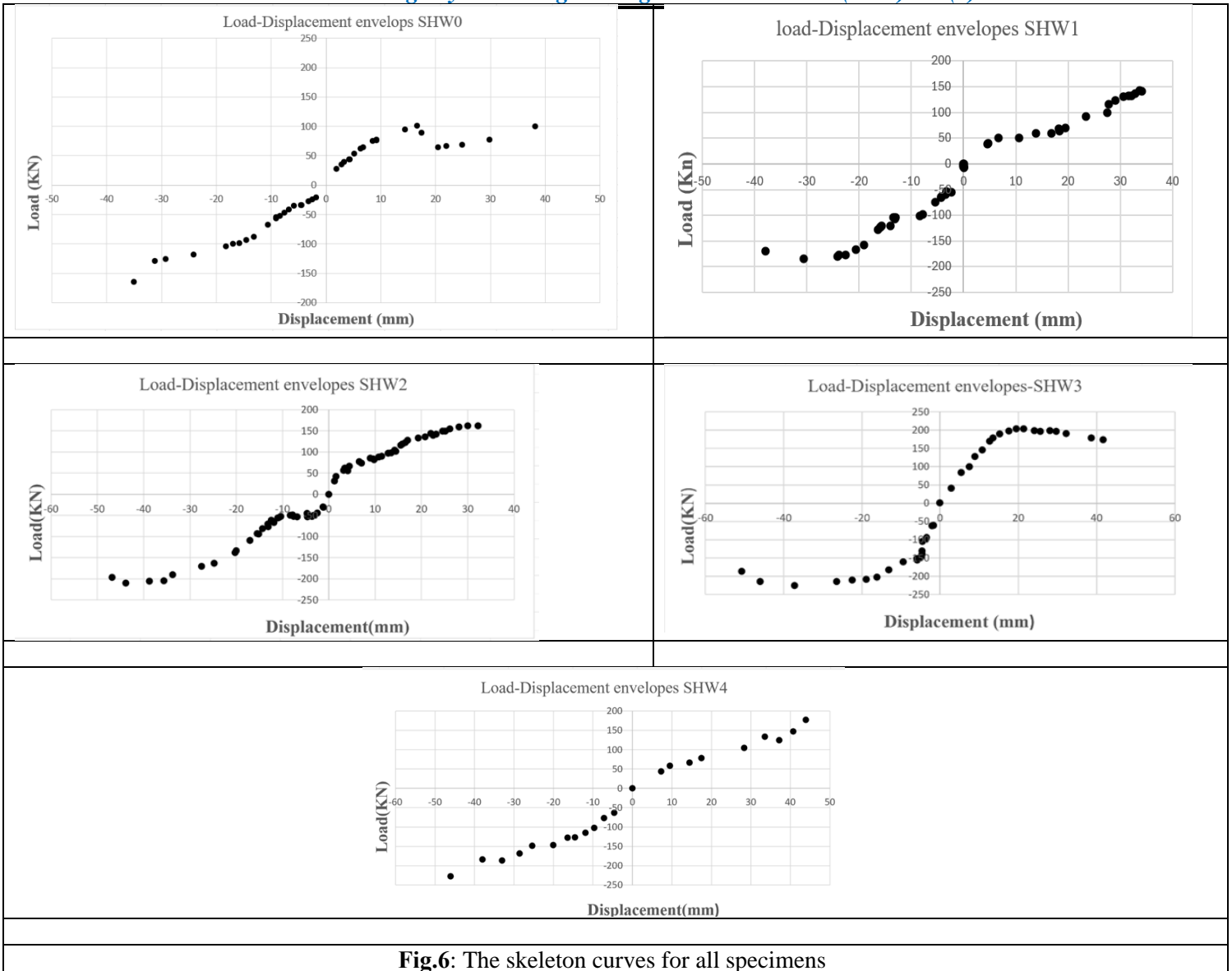
Fig.6: The skeleton curves for all specimens

3.4. Ductility Coefficient

Ductility is crucial when assessing earthquake performance. It refers to a structural feature that enables large deformations and the ability to absorb energy through hysteretic action, as discussed by Pauly and Priestly [18]. A displacement ductility ratio is used to assess a sample's deformation capabilities. Figure (8) shows that the point where they intersect is the tangential envelope curve's from the origin. The maximum (failure) load is defined by the largest load magnitude, which is decreased to 85% of the ultimate load, as well as the load at rapid sample failure. Ductility (μ) is the ratio of displacement at failure load to displacement at yielding load for a sample.

$$\mu = \frac{\Delta max}{\Delta yield}$$ (1)

Table (3) includes the values for Pu (ultimate load), Py (yielding load), Δy (displacement at yielding load), Δmax (displacement at failure load), and μ (ductility ratio). They were approximated with envelope curves for both positive and negative loads. The yielding point is calculated using Paul and Priestly's formula ($0.85 \times 0.7 \times$ Pu) [18].
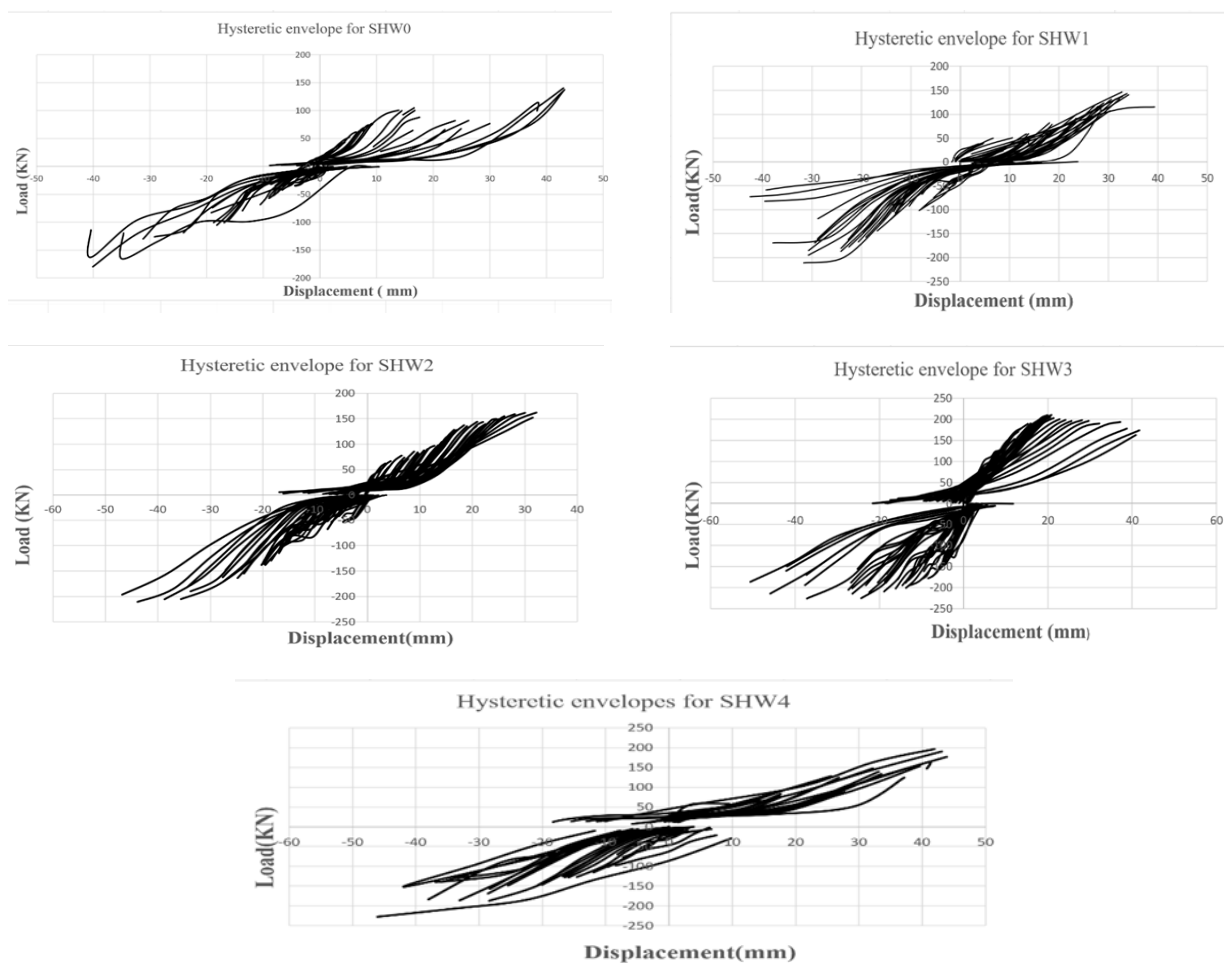
Fig. 7 The hysteresis envelope curves for positive and negative

3.5. Energy Dissipation

The damping index ηe measures the energy-dissipating capacity of shear wall samples. The required damping factor can be determined using the hysteresis. Loops in Figure (9) are defined as the regions contained by the loop of the hysteresis curve that indicate the non-elastic dissipating energy inside a full hysteresis loop. The energy dissipation capacity is measured using the equation [2], which takes into consideration the equivalent viscous damping coefficient ηe.

$$n_e = \frac{1 * A_{(abd+cdb)}}{2\pi \ A_{(Ola+OJc)}} \qquad (2)$$

Where:

$A_{(abd+cdb)}$: Area of load-displacement hysteretic loop at maximum load for both upward and downward sections.

$A_{(Oia+Ojc)}$: Area of triangles for both ascent and descent of loop at maximum load.
The area of triangles illustrates the greatest energy, i.e.,

$$E = P \times \Delta / 2 \quad (3)$$

Table (3): Ductility ratio μ and its percentage to control sample

Sample	Case of loading	Py	Δ_y	P$_u$	Δ_u	Failure	Δ_{max}	$\mu = \dfrac{\Delta max}{\Delta yield}$	$\dfrac{\Delta sample}{\Delta S1}$
SHW0	Push(-ve)	107	23.14	180	40	153	40	1.73	1.0
	Pull(+ve)	83.5	14.7	140	43	119	43	2.93	1.0
SHW1	Push (-ve)	125.545	23.5	211	31.7	179.35	31.7	1.35	0.78
	Pull (+ve)	87.465	23.48	147	32.7	124.95	32.7	1.39	0.474
SHW2	Push(-ve)	125.3	28.561	210.57	43.867	178.984	43.867	1.53	0.884
	Pull(+ve)	96.4	12.778	162.04	32.184	137.734	32.184	2.5	0.853
SHW3	Push(-ve)	134.6	4.754	226.18	37.2	192.3	37.2	9.3	5.375
	Pull (+ve)	125.12	9.004	210.28	20.86	187.7	20.86	2.32	0.79
SHW4	Push(-ve)	135.39	11.856	227.54	46.03	193.409	46.03	3.88	2.24
	Pull (+ve)	116.78	31.142	196.27	41.92	166.83	41.92	1.34	0.46

Table (4): The equivalent viscous damping coefficient ηe

Sample	Area of max. hysteresis loop	Area of max. energy (area of triangles)	Viscous damping coefficient(ηe)
SHW0	2306.424	6619.573	0.055431
SHW1	3089.1064	5735.384	0.085687
SHW2	4256.947	7226.085	0.0937218
SHW3	3839.815	6232.685	0.0980123
SHW4	7722.1416	8628.0443	0.1423871
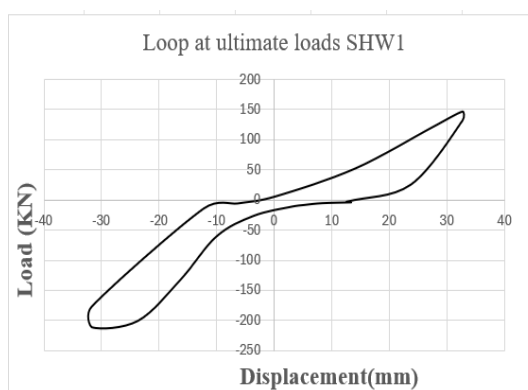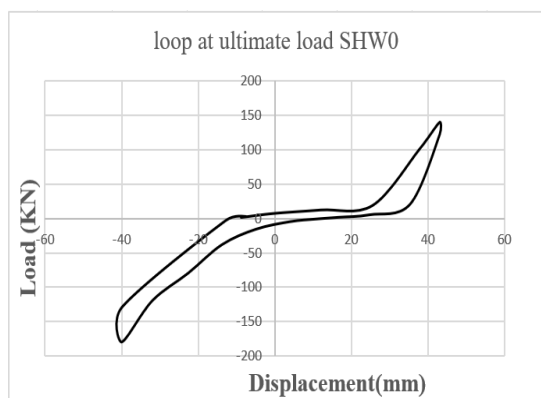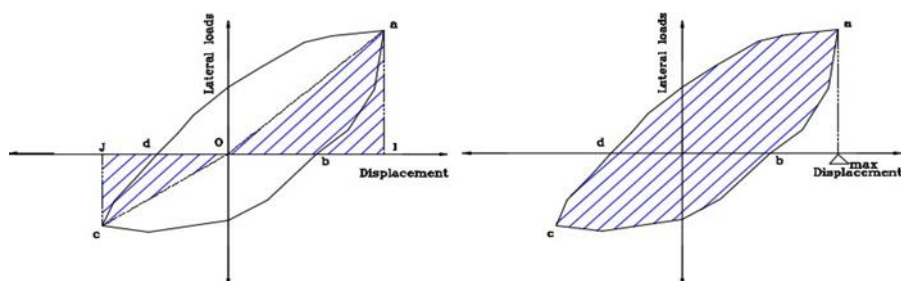
Fig. 8: The maximum hysteresis loop for calculating viscous damping coefficient ηe
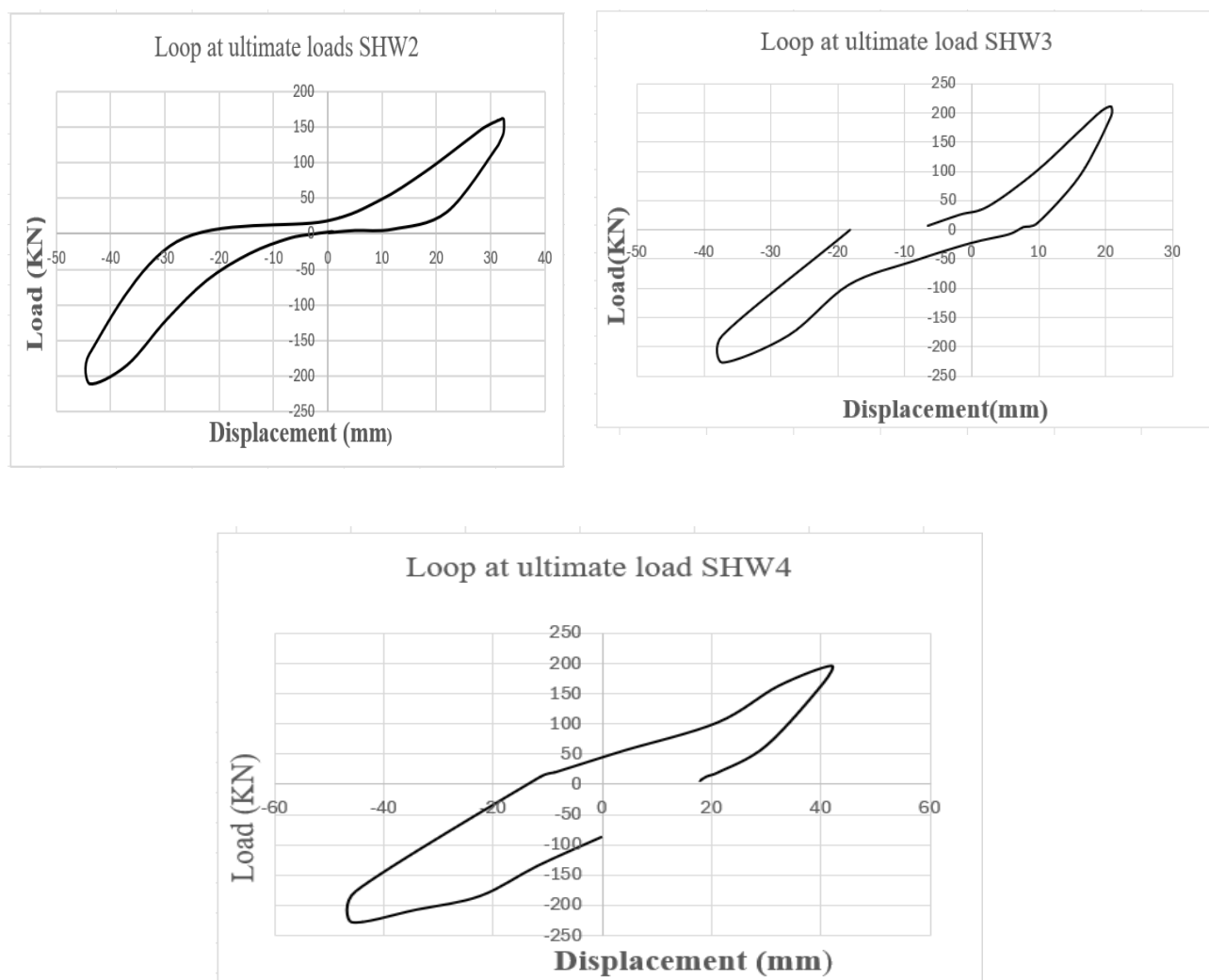
Cont. Fig. 8: The maximum hysteresis loop for calculating viscous damping coefficient ηe

SHW3 has the highest ductility ratio under push loading, with a value of 5.5, which is much greater than any other specimen. This suggests that SHW3 can sustain bigger deformations before failure, indicating superior energy absorption capacities and enhanced seismic performance.

Among the other specimens, SHW2 has a ductility ratio of 2.5 under push loading, which is 145% more than that of the control sample. This specimen has a higher energy dissipation capacity than SHW0. SHW1 and SHW4 exhibit the lowest ductility ratios under both push and pull loading situations, with values of 1.35 and 1.34 (push loading) and 1.39 and 1.46 (pull loading), respectively. The values provided are significantly less than those of SHW3, implying that these specimens would experience reduced deformation and energy dissipation capacity in comparison to SHW3 .

SHW0, as the control specimen, demonstrates baseline performance with ductility ratios of 1.73 and 2.93 for push and pull loading, respectively. In general, SHW4 demonstrates the most substantial energy dissipation, followed by SHW3 and SHW2. SHW1 likewise exhibits higher energy dissipation than SHW0, but to a minor level. The comparison demonstrates that the use of carbon fiber strengthening substantially improves the energy dissipation capability of the shear walls.

4. Conclusions

The following conclusions can be addressed based on experimental investigations.

- The performance of CFRP strengthened shear walls significantly improved when mechanical fasteners are incorporated.
- The shear walls strengthened with horizontal and X-pattern CFRP strips (SHW1 and SHW2) showed increased load capacity and displacement resistance, and SHW2 showed the highest improvement in strength and ductility.
- The incorporation of mechanical fasteners in addition to CFRP strips (SHW3 and SHW4), showed the most substantial improvements. SHW3, in particular, showed the highest load capacity and displacement resistance, as well as superior energy dissipation, attributable to the stabilization provided by the fasteners. The loops of hysteresis for SHW3 and SHW4 were less pinched, indicating increased energy absorption when compared with SHW1 and SHW2.
- The energy dissipation coefficients also revealed SHW4 as having the largest energy dissipation capacity, followed by SHW3, SHW2, SHW1, and SHW0.
- This trend indicates that as both the CFRP configuration and the mechanical fastening improve, the ability of the shear wall to release seismic energy additionally improves.
- In general, the use of CFRP strips, particularly when combined with mechanical fasteners, significantly improves the seismic resilience of shear walls, making them more effective at resisting deformation and absorbing energy under cyclic loading. SHW3 and SHW4 are particularly suitable for applications requiring high seismic protection due to its increased ductility, load capacity, and energy dissipation characteristics.

References

[1] Triantafillou, T. (1998). Strengthening of structures with advanced FRPs. Progress in Structural Engineering and Materials, 1, 126-134, https://doi.org/10.1002/PSE.2260010204.

[2] Priestley, M., Seible, F., & Calvi, G. (1996). Seismic Design and Retrofit of Bridges, https://doi.org/10.1002/9780470172858.

[3] Kawashima, K. (2000). Seismic design and retrofit of bridges. Bulletin of the New Zealand National Society for Earthquake Engineering, 33, 265-285, https://doi.org/10.5459/BNZSEE.33.3.265-285.

[4] Ehsani, M., & Saadatmanesh, H. (1997). Fiber Composites: An Economical Alternative for Retrofitting Earthquake-Damaged Precast-Concrete Walls. *Earthquake Spectra,* 13, 225 - 241. https://doi.org/10.1193/1.1585943.

[5] Lombard J, Lau D, Humar, J, Foo S, Cheung M. Seismic Strengthening and Repair of Reinforced Concrete Shear Walls. In: Paper No. 2032, Proceeding of the 12th world conference on earthquake engineering. New Zealand; 2000 (CD-ROM)

[6] Hsiao, F. P., Wang, J. C., & Chiou, Y. J. (2008). Shear strengthening of reinforced concrete framed shear walls using CFRP strips. In 14th World Conference on Earthquake Engineering.

[7] Layssi, H., & Mitchell, D. (2012, June). Experiments on seismic retrofit and repair of reinforced concrete shear walls. In *Proceedings of the 6th International Conference on FRP Composites in Civil Engineering (CICE)* (pp. 13-15).

[8] Layssi, H., Cook, W. D., & Mitchell, D. (2012). Seismic response and CFRP retrofit of poorly detailed shear walls. *Journal of Composites for Construction*, *16*(3),332-339. https://doi.org/10.1061/(ASCE)CC.1943-5614.0000259

[9] Altin, S., Anil, Ö., Kopraman, Y., & Kara, M. E. (2013). Hysteretic behavior of RC shear walls strengthened with CFRP strips. *Composites Part B: Engineering*, *44*(1), 321-329. https://doi.org/10.1016/j.compositesb.2012.05.009

[10] Cruz-Noguez, C. A., Lau, D. T., Sherwood, E. G., Hiotakis, S., Lombard, J., Foo, S., & Cheung, M.

(2015). Seismic behavior of RC shear walls strengthened for in-plane bending using externally bonded FRP sheets. *Journal of Composites for Construction*, *19*(1), 04014023. https://doi.org/10.1061/(ASCE)CC.1943-5614.0000478

[11] Woods, J. E., Lau, D. T., & Cruz-Noguez, C. A. (2016). In-plane seismic strengthening of nonductile reinforced concrete shear walls using externally bonded CFRP sheets. *Journal of Composites for Construction*, *20*(6), 04016052. https://doi.org/10.1061/(ASCE)CC.1943-5614.0000705

[12] Woods, J., Lau, D., Cruz-Noguez, C., & Shaheen, I. (2017). Repair of earthquake damaged squat reinforced concrete shear walls using externally bonded CFRP sheets. In *Proc., 16th World Conf. on Earthquake Engineering* (pp. 1-8).

[13] Husain, M., Eisa, A. S., & Hegazy, M. M. (2019). Strengthening of reinforced concrete shear walls with openings using carbon fiber-reinforced polymers. *International Journal of Advanced Structural Engineering*, *11*, 129-150.

[14] Neale KW, Demers M, DeVino B, Ho, NY. Strengthening of wall-type reinforced concrete columns with fibre-reinforced composite sheets. In: Lau Ong JM, Paramasivam P, editors. Structural failure, durability, and retrofitting, KCG. Singapore Concrete Institute; 1997. p. 410

[15] Iso M, Matsuzaki Y, Sonobe Y, Nakamura H, Watanabe M. Experimental study on reinforced concrete columns having wing walls retrofitted with continuous fiber sheets. In: Paper No. 1865, Proceeding of the 12th world conference on earthquake engineering. New Zealand; 2000 (CD-ROM).

[16] Sugiyama T. et al. Experimental study on the performance of the RC frame infilled cast-in-place nonstructural RC walls retrofitted by using carbon fiber sheets. In: Paper No. 2153, Proceeding of the 12th world conference on earthquake engineering. New Zealand; 2000 (CD-ROM).

[17] American Concrete Institute (ACI 318-19). Building Code Requirements for Structural Concrete and Commentary. Farmington Hills, MI, USA, 201,section10.3,Chapter22.

[18] Paulay, T. (1992). Seismic design of reinforced concrete and masonry buildings. *John Willey & Sons*.